Published in final edited form as:
Heart Rhythm. 2011 January ; 8(1): 48–55. doi:10.1016/j.hrthm.2010.09.010.

R231C mutation in *KCNQ1* causes long QT syndrome type 1 and familial atrial fibrillation

Daniel C. Bartos, BS[*], **Sabine Duchatelet, PhD**[†,‡], **Don E. Burgess, PhD**[*,§], **Didier Klug, MD**[‖], **Isabelle Denjoy, MD**[†,‡,¶], **Rachel Peat, PhD**[†,‡], **Jean-Marc Lupoglazoff, MD, PhD**[†,‡,#], **Véronique Fressart, MD, PhD**[†,‡,**], **Myriam Berthet, BA**[†,‡], **Michael J. Ackerman, MD, PhD**[††], **Craig T. January, MD, PhD**[‡‡], **Pascale Guicheney, PhD**[†,‡], and **Brian P. Delisle, PhD**[*]

[*]University of Kentucky, Lexington, Kentucky

[†]INSERM, U956, Hôpital Pitié-Salpêtrière, Paris, France

[‡]UPMC University of Paris 06, UMR_S956, IFR14, Paris, France

[§]Asbury College, Wilmore, Kentucky

[‖]Hôpital Cardiologique de Lille, Lille, France

[¶]Hôpital Lariboisière, Centre de Référence des Maladies Cardiaques Héréditaires, Paris, France

[#]Hôpital Robert-Debré, Paris, France

[**]UF Cardiogénétique et Myogénétique, Service de Biochimie B, Assistance Publique-Hôpitaux de Paris, Hôpital Pitié-Salpêtrière, Paris, France

[††]Mayo Clinic, Rochester, Minnesota

[‡‡]University of Wisconsin–Madison, Madison, Wisconsin

Abstract

BACKGROUND—Loss-of-function mutations in the gene *KCNQ1* encoding the Kv7.1 K^+ channel cause long QT syndrome type 1 (LQT1), whereas gain-of-function mutations are associated with short QT syndrome as well as familial atrial fibrillation (FAF). However, *KCNQ1* mutation pleiotropy, which is capable of expressing both LQT1 and FAF, has not been demonstrated for a discrete *KCNQ1* mutation. The genotype–phenotype relationship for a family with FAF suggests a possible association with the LQT1 p.Arg231Cys-KCNQ1 (R231C-Q1) mutation.

OBJECTIVE—The purpose of this study was to determine whether R231C-Q1 also can be linked to FAF.

METHODS—The R231C-Q1 proband with AF underwent genetic testing for possible mutations in 10 other AF-linked genes plus *KCNH2* and *SCN5A*. Sixteen members from five other R231C-positive LQT1 families were genetically tested for 21 single nucleotide polymorphisms (SNPs) to determine if the FAF family had discriminatory SNPs associated with AF. R231C-Q1 was expressed with KCNE1 (E1) in HEK293 cells, and Q1E1 currents (I_{Q1E1}) were analyzed using the whole-cell patch-clamp technique.

Address reprint requests and correspondence: Dr. Brian P. Delisle, University of Kentucky, 800 Rose St. MS508, Lexington, Kentucky 40503. brian.delisle@uky.edu.

RESULTS—Genetic analyses revealed no additional mutations or discriminatory SNPs. Cells expressing WT-Q1 and R231C-Q1 exhibited some constitutively active I_{Q1E1} and smaller maximal I_{Q1E1} compared to cells expressing WT-Q1.

CONCLUSION—Constitutively active I_{Q1E1} and a smaller peak I_{Q1E1} are common features of FAF-associated and LQT1-associated mutations, respectively. These data suggest that the mixed functional properties of R231C-Q1 may predispose some families to LQT1 or FAF. We conclude that R231C is a pleiotropic missense mutation capable of LQT1 expression, AF expression, or both.

Keywords

Atrial fibrillation; Familial atrial fibrillation; Genetics; Ion channel; KCNQ1; Long QT syndrome; Long QT syndrome type 1

Introduction

Atrial fibrillation (AF) is the most common cardiac arrhythmia affecting 10% of the population by the age of 75 years.[1] The disease can present as lone AF; however, AF usually is associated with underlying heart disease, hypertension, or hyperthyroidism. Approximately 30% of AF patients have parents with a history of AF, suggesting a genetic predis-position. [2]

Loss-of-function mutations in *KCNQ1* cause long QT syndrome type 1 (LQT1, MIM#192500), whereas gain-of-function mutations have been implicated in short QT syndrome (SQTS, MIM#609621) and familial atrial fibrillation (FAF, MIM#607554) (for review, see references [3–7]). *KCNQ1* encodes the voltage-gated K^+ channel α-subunit 7.1 (Kv7.1). In the heart, KCNQ1 channels (Q1) co-assemble with KCNE1 β-subunits (E1), forming a channel that generates the slowly activating delayed rectifier K^+ current I_{Ks}.[8,9] Heterologous expression of Q1 and E1 generate currents (I_{Q1E1}) that recapitulate native-like I_{Ks}.

Several groups have implicated the missense mutation annotated as p.Arg231Cys (R231C-Q1) in LQT1, druginduced long QT syndrome (LQTS) with AF, fetal bradycardia, and persistent AF where QTc prolongation was noted after cardioversion.[10–15] We now report the genotype– phenotype relationships for six R231C-positive families, five of which have LQTS and one family containing four R231C-positive individuals affected by lone AF before age 50 years. Functional analyses suggest that co-expression of wild-type Q1 (WT-Q1) and R231C-Q1 exhibited a mixed functional phenotype that has both loss-of-function (LQT1) and gain-of-function (FAF) properties. This is the first study to demonstrate pleiotropy in *KCNQ1* whereby a discrete missense mutation is capable of both LQT1 and FAF expressivity using genetic and functional analyses.

Methods

Study population and diagnostic criterion

Patients enrolled were probands referred for genetically linked arrhythmias or fetal bradycardia. Blood samples were obtained from family members who agreed to genetic evaluation and provided written consent. Patients underwent clinical evaluation and cardiovascular examination, including 12-lead ECG and 24-hour Holter recording. Lone AF was diagnosed in patients with AF and normal thyroid function, no hypertension, or structural disease as determined by echocardiography. Prolonged QTc was diagnosed based on prolongation of ventricular repolarization at rest in lead II corrected QT interval (QTc)

>440 ms for males and >460 ms for females using the Bazett formula (QTc for R231C-Q1 subjects are given in Online Supplemental Table 1). The R231C subjects with fetal bradycardia were previously reported.[11]

Genetic analysis

Genomic DNA was extracted from peripheral blood leukocytes using standard methods. Mutational analyses of *KCNQ1, KCNH2, KCNE1*, and *SCN5A* genes were performed in probands. The coding regions were amplified using polymerase chain reaction and sequenced with a 3100 BigDye Terminator v3.1 sequencing kit and ABI PRISM 3100 Genetic Analyzer (Applied Biosystems, Foster City, CA, USA). We sequenced other AF-linked genes [*KCNE2* (NM172201), *KCNE3* (NM005472), *KCNE5* (NM012282), *NPPA* (NM006172), *KCNA5* (NM002234), *KCNJ2* (NM00891), *GJA5* (NM005266 and 181703), *SCN1B* (NM001037 and 199037), *SCN2B* (NM004588)] and *SCN3B* (NM018400) in the R231C-Q1 proband from the family with AF (Figure 1, Family A, subject II:1) (for review, see reference [16–20]). We also compared 21 single nucleotide polymorphisms (SNPs) (including *KCNE5*) that alter AF susceptibility (rs1805123, rs1805120, rs1805127, rs1805124, rs2200733, rs10033464, rs35594137, rs12621643, rs1800872, rs583362, rs7193343, rs3807989, rs11708996, rs6800541, rs251253, rs5063, rs13376333, rs11047543, rs3825214, rs1801252, and rs17003955) among the families shown in Figure 1 (Online Supplemental Table 2).

Tissue culture and electrophysiology

Mutagenesis and transfection are described in the Online Supplemental Methods. Human embryonic kidney 293 (HEK293) cells transfected with WT-Q1 (3 μg) plasmid DNA expressed small currents that did not resemble I_{Ks}. Cells expressing R231C-Q1 (3 μg) plasmid DNA also expressed small currents that appeared constitutively active (Online Supplemental Figure 1). To recapitulate I_{Ks}-like currents, we transfected cells with equal amounts of E1 (3 μg) and Q1 (3 μg) plasmid DNA (total concentration 6 μg). Because of the differences in size of E1 and Q1 cDNA, the final ratio of E1 to Q1 cDNA ratio is ~2:1. For co-expression studies with WT-Q1 and mutant Q1 cDNA, equal amounts of WT-Q1 (1.5 μg) and mutant Q1 (1.5 μg) were used to maintain the equivalent Q1 plasmid concentrations (3 μg) (see Online Supplemental Methods for electrophysiologic techniques). pCLAMP 10 software (Axon Instruments, Union City, CA, USA) was used to generate the voltage protocols, acquire current signals, and data analyses. Origin (7.0, Microcal, Northhampton, MA, USA) was used for performing Boltzmann curve fitting to the current–voltage (I–V) relations and for generating graphs. Data were fit using the following Boltzmann equation:

$$I=(I_{MIN}-I_{MAX})/(1+e^{(V-V_{\frac{1}{2}})/k})+I_{MAX}$$

where I_{MIN} = minimally activated current, I_{MAX} = maximally activated current, $V_{1/2}$ = midpoint potential for half-maximal activation, and k = slope factor. For most experiments, the holding potential was −80 mV, and the dashed line in figures is the zero current. The physiologic temperature and action potential (AP) clamp measurements were done similar to that previously described.[21]

Computational modeling

Computational models of human atrial and ventricular action potentials were used and are described in detail in the Online Supplemental Methods.[20,22]

Statistical analysis

Analysis of variance was performed on datasets. $P < .05$ was considered significant. We subsequently performed t-tests to identify which experimental group(s) differed from one another.

Results

R231C-Q1 is linked to LQTS, fetal bradycardia, and AF

We identified R231C-Q1 in six probands with various clinical phenotypes (Figure 1), including one with AF (Family A), three neonates with fetal bradycardia (Families B, D, E),[11] one with prolonged QTc (Family F), and one who is a member of a large LQTS family previously linked to chromosome 11p15 (Family C).[23] Although the Family C proband (I:2) is asymptomatic, several other family members are symptomatic for LQTS (not shown), including the baby from her niece who was diagnosed with fetal LQTS and bradycardia resulting in intrauterine death at full term.[23]

In Family A, AF was diagnosed in the female proband (II:1) at age 33 years, in her father (I:1) at age 18 years, and in two of her brothers (II:3, II:5) at age 30 years and 15 years, respectively. The proband was hospitalized when she was 33 years old for persistent AF that occurred during stress. After an electrical cardioversion, she has been treated by sotalol without clinical recurrences for 3 years (Online Supplemental Figure 2). Paroxysmal AF then occurred, and sotalol treatment was replaced by flecainide without clinical recurrences of AF. In contrast to the other R231C-positive LQTS families, patients of Family A do not manifest either QTc prolongation or syncope except for patient II:5, who had ventricular fibrillation 4 months after interruption of sotalol treatment and died of severe cerebral anoxic damage several days later at age 22 years. In addition, one of the R231C-positive brothers (II:4) thus far is asymptomatic for AF at age 37 years. None of the R231C- and AF-positive subjects in Family A have structural heart disease, hypertension, or hyperthyroidism consistent with a clinical diagnosis of lone AF. Furthermore, genetic testing of the proband (II:1) did not reveal any additional mutations in other AF susceptibility genes.

The members of Families B through E do not present with AF, including the proband of Family F, now age 57 years, who currently is receiving beta-blocker treatment and underwent defibrillator implantation 3 years ago following a severe LQTS-triggered cardiac event. Suspecting the possible contribution of additional genetic factors to AF development, we genotyped all the family members for 21 different SNPs that confer some AF susceptibility (Online Supplemental Table 2). We did not find any obvious differences between Family A and Families B–F that might account for their different clinical phenotypes, except for possibly rs251253, an intergenic SNP located in the region of *NKX2-5* gene encoding a cardiac-specific homeobox transcription factor. Indeed, in Family A, only the son with the R231C-Q1 mutation who did not have AF carries the protective allele. All of the mutation carriers from the five additional R231C-positive LQTS families have the protective allele, with the exception of the patient II:2 from Family C (a woman who does not manifest AF at age 33 years). We conclude that R231C-Q1 is linked to LQTS, fetal bradycardia, and lone AF.

R231C-Q1 results in large constitutively activated I_{Q1E1}

We tested the hypothesis that R231C-Q1 may generate a unique functional phenotype compared to other LQT1 mutations that typically result in a loss of function. We chose to study the LQT1 mutation E160K-Q1 as a “positive control” because studies suggest that, like most LQT1-linked mutations, E160K-Q1 causes a loss of I_{Q1E1}.[24] Figure 2A shows representative families of whole-cell current traces recorded from nontransfected HEK293

cells and from cells expressing E1 and E160K-Q1 or R231C-Q1. The currents from nontransfected cells and from cells transfected with E160K-Q1 were measured by applying "step" pulses from −80 to 70 mV in 10-mV increments for 5 seconds, followed by a "tail" pulse to −50 mV for 5 seconds. At positive step pulses, nontransfected cells expressed a small endogenous outward current that was absent during the tail pulse. As expected, cells expressing E160K-Q1 did not generate any I_{Q1E1}. We attempted to use the same voltage protocol to measure I_{Q1E1} from cells expressing R231C-Q1, but R231C-Q1 was constitutively active and generated very large I_{Q1E1} that could not be measured reliably because of apparent changes in local $[K^+]$ (data not shown). We minimized these effects by shortening the duration of the step and tail pulses to 50 ms and 150 ms, respectively. The large constitutively active I_{Q1E1} measured from cells expressing R231C-Q1 was clarified by applying step pulses from −120 to 70 mV in 10-mV increments, followed by a tail pulse to −50 mV (Figure 2A). Figures 2B and 2C show the mean peak step and tail I–V relations, respectively, for nontransfected cells (n = 10), cells expressing E160K-Q1 (n = 8), and cells expressing R231C-Q1 (n = 20). Although E160K-Q1 and R231C-Q1 both are linked to LQT1, their effects on I_{Q1E1} are dramatically different from one another.

Co-expression of WT-Q1 and R231C-Q1 yields a mixed functional phenotype

LQT1 and FAF follow a dominant inheritance pattern; therefore, we determined the effect of co-expressing WT-Q1 and E160K-Q1 or R231C-Q1. Figure 3A shows representative families of whole-cell currents measured from cells expressing E1 with WT-Q1, WT-Q1 and E160KQ1, or WT-Q1 and R231C-Q1. The currents were measured using the 5-second voltage protocol described in Figure 2. Cells expressing WT-Q1 showed I_{Q1E1} that resembled native I_{Ks}. Cells expressing WT-Q1 and E160K-Q1 showed I_{Q1E1} with similar characteristics as I_{Ks}, but the amplitudes were smaller than cells expressing WT-Q1. Cells expressing WT-Q1 and R231C-Q1 showed I_{Q1E1} that had a mixed functional phenotype, some constitutively active I_{Q1E1} and some voltage-dependent I_{Q1E1}. Figures 3B and 3C show the mean peak I–V relations measured during the step and tail pulse, respectively, for cells expressing WT-Q1 (n = 31), WT-Q1 and E160K-Q1 (n = 13), or WT-Q1 and R231C-Q1 (n = 22). Mean peak tail I_{Q1E1} data were described using the Boltzmann function to calculate I_{MIN}, I_{MAX}, $V_{1/2}$, and k for I_{Q1E1} activation. Figure 3D shows that cells expressing WT-Q1 and R231C-Q1 had the largest mean I_{MIN} (which likely reflected their constitutively active component of I_{Q1E1}), but cells expressing WT-Q1 had the largest mean I_{MAX} (Figure 3D). Cells expressing WT-Q1 and R231C-Q1 had a more negative $V_{1/2}$ (Figure 3E), but k was not different (Figure 3F).

The data demonstrate that, compared to cells expressing WT-Q1 or R231C-Q1 (Figure 2), cells expressing WT-Q1 and R231C-Q1 had the smallest peak I_{Q1E1}. This may be related to alterations in the cell surface expression; however, when performed, biotinylation assays did not reveal significant differences in the relative amount of Q1 at the cell surface (see Online Supplemental Figure 3).

To measure the constitutively active component of I_{Q1E1} from cells expressing WT-Q1 and R231C-Q1, we used a voltage protocol similar to that used to measure I_{Q1E1} from cells expressing R231C-Q1 (Figure 2). Figure 4A shows representative families of I_{Q1E1} from cells expressing E1 and WT-Q1 or WT-Q1 and R231C-Q1. I_{Q1E1} was measured by applying 50-ms step pulses from −120 to −10 mV in 10-mV increments, followed by a 150-ms tail pulse to −50 mV. Figures 4B and 4C show the mean peak step and tail I–V relations, respectively, for cells expressing WT-Q1 (n = 11) or cells expressing WT-Q1 and R231C-Q1 (n = 13). Cells expressing WT-Q1 showed almost no I_{Q1E1}, whereas cells expressing WT-Q1 and R231C-Q1 showed constitutively active I_{Q1E1}.

Thus far, the data suggest that R231C-Q1 more closely resembles an FAF mutation and not an LQT1 mutation.[5,7] To understand how R231C-Q1 may contribute to an LQT1 phenotype, we measured currents from nontransfected cells, and cells expressing E1 and WT-Q1 or WT-Q1 and R231C-Q1 at 37°C using a ventricular AP waveform pulsed at 1 Hz. Figure 4D shows the AP potential waveform and representative averaged currents for 1 minute. The small current measured from nontransfected cells is a combination of endogenous HEK current and uncompensated leak and capacitative currents. Cells expressing WT-Q1 or WT-Q1 and R231C-Q1 showed large currents that both peaked during the plateau phase. Compared to cells expressing WT-Q1, cells expressing WT-Q1 and R231C-Q1 did not alter the mean peak current measured during the action potential waveform (WT-Q1 = 371 ± 162 pA/pF, n = 6; and WT-Q1 and R231C-Q1= 335 ± 171 pA/pF, n = 5, respectively), but cells expressing WT-Q1 and R231C-Q1 reduced the fraction of current that remained after repolarization to diastolic potentials (WT-Q1 = 0.14 ± 0.03, and WT-Q1 and R231C-Q1 = 0 ± 0.03). The latter effect is consistent with an LQT1 phenotype.

Discussion

This is the first study to link a known LQT1 mutation (R231C) to FAF and to show that an LQT1 mutation can generate a functional phenotype similar to the other *KCNQ1*-mediated FAF mutations.[5,7] We sequenced most of the known AF-associated genes in the R231C-Q1 AF proband but did not identify any additional mutations. Twentyfour subjects from six R231C-Q1 families were genotyped for 21 SNPs described as being at risk or protective for AF. These analyses (see Online Supplemental Table 2) may have identified a specific allele, *NKX2-5*, that discriminates AF from LQTS patients. The cardiac homeobox Nkx2-5 protein is essential in cardiac development, and mutations in *NKX2-5* cause various congenital heart malformations. Interestingly, Nkx2.5 regulates the transcription of *NPPA*, a gene in which mutations cause AF.[20]

R231C-Q1 generated constitutively active I_{Q1E1} similar to the FAF-associated *KCNQ1* mutations S140G and V141M.[5,7] Restier et al[25] suggest that these mutations alter charge–pair interactions between E160, R231, and R237 to cause ultraslow deactivation and generate the constitutively active I_{Q1E1} phenotype. A proposed structural model for a closed Q1 channel is shown in Figure 5A,[26] and this model suggests that the side chains of S140 and E160 are within van der Waals contact of R231 in the closed state. Perhaps R231C-Q1 mimics the effects that S140G-Q1 or V141M-Q1 have on charge–pairing interactions to generate I_{Q1E1} with a constitutively active phenotype. This structural model implies that this Q1 domain is a “hotspot” for mutations associated with multiple types of arrhythmia syndromes, including LQTS, fetal sinus bradycardia, and AF.

Prior to this study, two unrelated R231C-Q1 carriers were described with AF, one was a 72-year-old woman with an increased susceptibility to drug-induced LQTS, and the other was an unrelated 58-year-old woman who showed a prolonged QT interval after cardioversion.[14,15] Although it is tempting to speculate that R231C-Q1 underlies their AF phenotype, subsequent genetic analyses and the genotype– phenotype relationships of their families were not reported.

Consistent with an LQT1 phenotype, cells expressing WT-Q1 and R231C-Q1 reduced I_{Q1E1} during the repolarization phase of the ventricular action potential waveform (Figure 4D). Itoh et al[15] showed that cells expressing WT-Q1 and R231C-Q1 reduce maximal I_{Q1E1} by levels similar to that reported here (~50%, Figure 3D), and that reducing I_{Ks} by ~50% prolonged the duration in a Luo-Rudy model of a ventricular AP. Interestingly, experimental evidence from undiseased human ventricular myocytes suggest that basal I_{Ks} is small, and pharmacologic block of I_{Ks} by chromanol 293B does not alter human ventricular AP

duration.[27,28] The existence of LQT1 suggests that I_{Ks} can contribute to human ventricular repolarization under certain physiologic conditions, for example, with sympathetic tone, and the Luo-Rudy model may be helpful for modeling such conditions.

Grandi et al[22] recently developed a novel model of the human ventricular AP (the Grandi-Pasqualini-Bers [GPB] model). Similar to the experimental evidence, the model predicts only 1% to 3% prolongation with complete block of I_{Ks} in cells pulsed over a broad range of pacing cycle lengths. For didactic purposes, we modeled the mixed functional phenotype using a human atrial AP model and the GPB model (Figures 5B and 5C).[20,22] Both models were adjusted to reduce the number of functional I_{Ks} channels by ~50% and contain a constitutively active I_{Ks} component at 6.25% (the predicted fraction of homomeric mutant channels assuming random co-assembly). At a 1-Hz pacing rate, the modified I_{Ks} reduced the atrial AP duration by >50% and the ventricular AP duration by <1%. Modeling the constitutively active I_{Ks} component alone, without reducing the fraction of functional channels, had a similar effect: it shortened the atrial AP by >50% and the ventricular AP by <2% (Online Supplemental Figure 4). The constitutively active component selectively alters the atrial AP duration because the atrial AP is less positive and the atrial myocytes have a larger I_{Ks} density.[29] The modeling suggests that a small increase in the open probability of I_{Ks} channels will result in much larger I_{Ks} in atrial myocytes. This may explain why some AF-linked *KCNQ1* mutations that increase open probability do not always shorten QT-intervals. [5,30,31] Of note, early-onset AF (age <50 years) was reported in 2% of patients with genetically proven LQT1 compared to a background population prevalence of 0.1%.[32] This study raises the intriguing possibility that some of these LQT1 mutations may generate a mixed functional phenotype similar to R231C-Q1.

R231C-Q1 represents the first discrete missense mutation in the *KCNQ1*-encoded I_{Ks} potassium channel capable of pleiotropic expression. This is akin to the E1784K missense mutation in the *SCN5A*-encoded Nav1.5 sodium channel where E1784K not only is the most common *SCN5A* missense mutation responsible for LQTS type 3,[33] but it also is the most common type 1 Brugada syndrome-associated mutation.[34,35] The genetic, epigenetic, and environmental factors that drive a R231C-positive host or a E1784K-positive host to express one arrhythmia phenotype over the other remain elusive.

Study limitations

Unidentified factors may account for the different clinical phenotypes among R231C-Q1 families, and these data were obtained with a widely used heterologous overexpression system that could differ in native myocytes.

Conclusion

This is the first study to link a known LQT1 mutation to FAF. R231C-Q1 generates I_{Q1E1} with a mixed functional phenotype when co-expressed with WT-Q1: a constitutively active component with a smaller maximal I_{Q1E1}. This mixed functional phenotype may predispose R231C-Q1 families to multiple clinical phenotypes, including LQTS, fetal bradycardia, and/or AF.

Supplementary Material

Refer to Web version on PubMed Central for supplementary material.

Acknowledgments

This work was supported by National Heart Lung and Blood Institute Grant T32 HL072743 to Daniel Bartos; National Heart Lung and Blood Institute Grant R01 HL60723 to Dr. January; National Heart Lung and Blood Institute Grant R01 HL087039 to Dr. Delisle; Région Ile-de-France fellowships to Dr. Duchatelet; European Commission Grant 221685 to Drs. Guicheney and Peat; and Fédération and Société Françaises de Cardiologie to Drs. Denjoy and Guicheney.

ABBREVIATIONS

AF	atrial fibrillation
AP	action potential
E1	KCNE1
HEK293	human embryonic kidney 293
$\mathbf{I_{Ks}}$	slowly activating delayed rectifier K^+ current
$\mathbf{I_{MAX}}$	maximally activated current
$\mathbf{I_{MIN}}$	minimally activated current
$\mathbf{I_{Q1E1}}$	Q1E1 current
I–V	current–voltage
k	slope factor
LQT1	long QT syndrome type 1
LQTS	long QT syndrome
Q1	KCNQ1
SNP	single nucleotide polymorphism
$\mathbf{V_{1/2}}$	potential for half-maximal activation
WT	wild type

Appendix

Supplementary data

Supplementary data associated with this article can be found, in the online version, at doi:10.1016/j.hrthm.2010.09.010.

References

1. Conen D, Osswald S, Albert CM. Epidemiology of atrial fibrillation. Swiss Med Wkly. 2009; 39:346–352. [PubMed: 19562528]
2. Fox CS, Parise H, D'Agostino RB Sr, et al. Parental atrial fibrillation as a risk factor for atrial fibrillation in offspring. JAMA. 2004; 291:2851–2855. [PubMed: 15199036]
3. Lehnart SE, Ackerman MJ, Benson DW Jr, et al. Inherited arrhythmias: a National Heart, Lung, and Blood Institute and Office of Rare Diseases workshop consensus report about the diagnosis, phenotyping, molecular mechanisms, and therapeutic approaches for primary cardiomyopathies of gene mutations affecting ion channel function. Circulation. 2007; 116:2325–2345. [PubMed: 17998470]
4. Wang Q, Curran ME, Splawski I, et al. Positional cloning of a novel potassium channel gene: KVLQT1 mutations cause cardiac arrhythmias. Nat Genet. 1996; 12:17–23. [PubMed: 8528244]

5. Chen YH, Xu SJ, Bendahhou S, et al. KCNQ1 gain-of-function mutation in familial atrial fibrillation. Science. 2003; 299:251–254. [PubMed: 12522251]
6. Bellocq C, van Ginneken AC, Bezzina CR, et al. Mutation in the KCNQ1 gene leading to the short QT-interval syndrome. Circulation. 2004; 109:2394–2397. [PubMed: 15159330]
7. Hong K, Piper DR, Diaz-Valdecantos A, et al. De novo KCNQ1 mutation responsible for atrial fibrillation and short QT syndrome in utero. Cardiovasc Res. 2005; 68:433–440. [PubMed: 16109388]
8. Barhanin J, Lesage F, Guillemare E, Fink M, Lazdunski M, Romey G. KvLQT1 and IsK (minK) proteins associate to form the I_{Ks} cardiac potassium channel. Nature. 1996; 384:78–80. [PubMed: 8900282]
9. Sanguinetti MC, Curran ME, Zou A, Shen J, et al. Coassembly of KvLQT1 and minK (IsK) proteins to form cardiac I_{Ks} potassium channel. Nature. 1996; 384:80–83. [PubMed: 8900283]
10. Fodstad H, Swan H, Laitinen P, et al. Four potassium channel mutations account for 73% of the genetic spectrum underlying long-QT syndrome (LQTS) and provide evidence for a strong founder effect in Finland. Ann Med. 2004; 36S:53–63. [PubMed: 15176425]
11. Lupoglazoff JM, Denjoy I, Villain E, et al. Long QT syndrome in neonates: conduction disorders associated with HERG mutations and sinus bradycardia with KCNQ1 mutations. J Am Coll Cardiol. 2004; 43:826–830. [PubMed: 14998624]
12. Millat G, Chevalier P, Restier-Miron L, et al. Spectrum of pathogenic mutations and associated polymorphisms in a cohort of 44 unrelated patients with long QT syndrome. Clin Genet. 2006; 70:214–227. [PubMed: 16922724]
13. Basavarajaiah S, Wilson M, Whyte G, Shah A, Behr E, Sharma S. Prevalence and significance of an isolated long QT interval in elite athletes. Eur Heart J. 2007; 28:2944–2949. [PubMed: 17947213]
14. Zienciuk A, Szwoch M, Raczak G. Atrial fibrillation in the long QT syndrome. Kardiol Pol. 2009; 67:681–684. [PubMed: 19618328]
15. Itoh H, Sakaguchi T, Ding WG, et al. Latent genetic backgrounds and molecular pathogenesis in drug-induced long-QT syndrome. Circ Arrhythm Electrophysiol. 2009; 2:511–523. [PubMed: 19843919]
16. Fatkin D, Otway R, Vandenberg JI. Genes and atrial fibrillation: a new look at an old problem. Circulation. 2007; 116:782–792. [PubMed: 17698744]
17. Zhang DF, Liang B, Lin J, Liu B, Zhou QS, Yang YQ. KCNE3 R53H substitution in familial atrial fibrillation. Chin Med J (Engl). 2005; 118:1735–1738. [PubMed: 16313760]
18. Ravn LS, Aizawa Y, Pollevick GD, et al. Gain of function in I_{Ks} secondary to a mutation in KCNE5 associated with atrial fibrillation. Heart Rhythm. 2008; 5:427–435. [PubMed: 18313602]
19. Watanabe H, Darbar D, Kaiser DW, et al. Mutations in sodium channel beta1- and beta2-subunits associated with atrial fibrillation. Circ Arrhythm Electrophysiol. 2009; 2:268–275. [PubMed: 19808477]
20. Abraham RL, Yang T, Blair M, Roden DM, Darbar D. Augmented potassium current is a shared phenotype for two genetic defects associated with familial atrial fibrillation. J Mol Cell Cardiol. 2010; 48:181–190. [PubMed: 19646991]
21. Zhou Z, Gong Q, Ye B, et al. Properties of HERG channels stably expressed in HEK 293 cells studied at physiological temperature. Biophys J. 1998; 74:230–241. [PubMed: 9449325]
22. Grandi E, Pasqualini FS, Bers DM. A novel computational model of the human ventricular action potential and Ca transient. J Mol Cell Cardiol. 2010; 48:112–121. [PubMed: 19835882]
23. Desmyttere S, Bonduelle M, DeWolf D, Liebaers I, Lissens W. A case of term mors in utero in a chromosome 11P linked long QT family. Genetic Counsel. 1994; 5:289–295.
24. Silva JR, Pan H, Wu D, et al. A multiscale model linking ion-channel molecular dynamics and electrostatics to the cardiac action potential. Proc Natl Acad Sci U S A. 2009; 106:11102–11106. [PubMed: 19549851]
25. Restier L, Cheng L, Sanguinetti MC. Mechanisms by which atrial fibrillation-associated mutations in the S1 domain of KCNQ1 slow deactivation of I_{Ks} channels. J Physiol. 2008; 586:4179–4191. [PubMed: 18599533]

26. Kang C, Tian C, Sönnichsen FD, et al. Structure of KCNE1 and implications for how it modulates the KCNQ1 potassium channel. Biochemistry. 2008; 47:7999–8006. [PubMed: 18611041]
27. Virág L, Iost N, Opincariu M, et al. The slow component of the delayed rectifier potassium current in undiseased human ventricular myocytes. Cardiovasc Res. 2001; 49:790–797. [PubMed: 11230978]
28. Jost N, Virág L, Bitay M, et al. Restricting excessive cardiac action potential and QT prolongation: a vital role for I_{Ks} in human ventricular muscle. Circulation. 2005; 112:1392–1399. [PubMed: 16129791]
29. Wang Z, Fermini B, Nattel S. Rapid and slow components of delayed rectifier current in human atrial myocytes. Cardiovasc Res. 1994; 28:1540–1546. [PubMed: 8001043]
30. Seebohm G. Kv7.1 in atrial fibrillation. Heart Rhythm. 2009; 6:1154–1155. [PubMed: 19560405]
31. Das S, Makino S, Melman YF, et al. Mutation in the S3 segment of KCNQ1 results in familial lone atrial fibrillation. Heart Rhythm. 2009; 6:1146–1153. [PubMed: 19632626]
32. Johnson JN, Tester DJ, Perry J, Salisbury BA, Reed CR, Ackerman MJ. Prevalence of early-onset atrial fibrillation in congenital long QT syndrome. Heart Rhythm. 2008; 5:704–709. [PubMed: 18452873]
33. Kapplinger JD, Tester DJ, Salisbury BA, et al. Spectrum and prevalence of mutations from the first 2,500 consecutive unrelated patients referred for the FAMILION long QT syndrome genetic test. Heart Rhythm. 2009; 6:1297–1303. [PubMed: 19716085]
34. Kapplinger JD, Tester DJ, Alders M, et al. An international compendium of mutation in the SCN5A-encoded cardiac sodium channel in patients referred for Brugada syndrome genetic testing. Heart Rhythm. 2010; 1:33–46. [PubMed: 20129283]
35. Makita N, Behr E, Shimizu W, et al. The E1784K mutation in SCN5A is associated with mixed clinical phenotype of type 3 long QT syndrome. J Clin Invest. 2008; 118:2219–2229. [PubMed: 18451998]

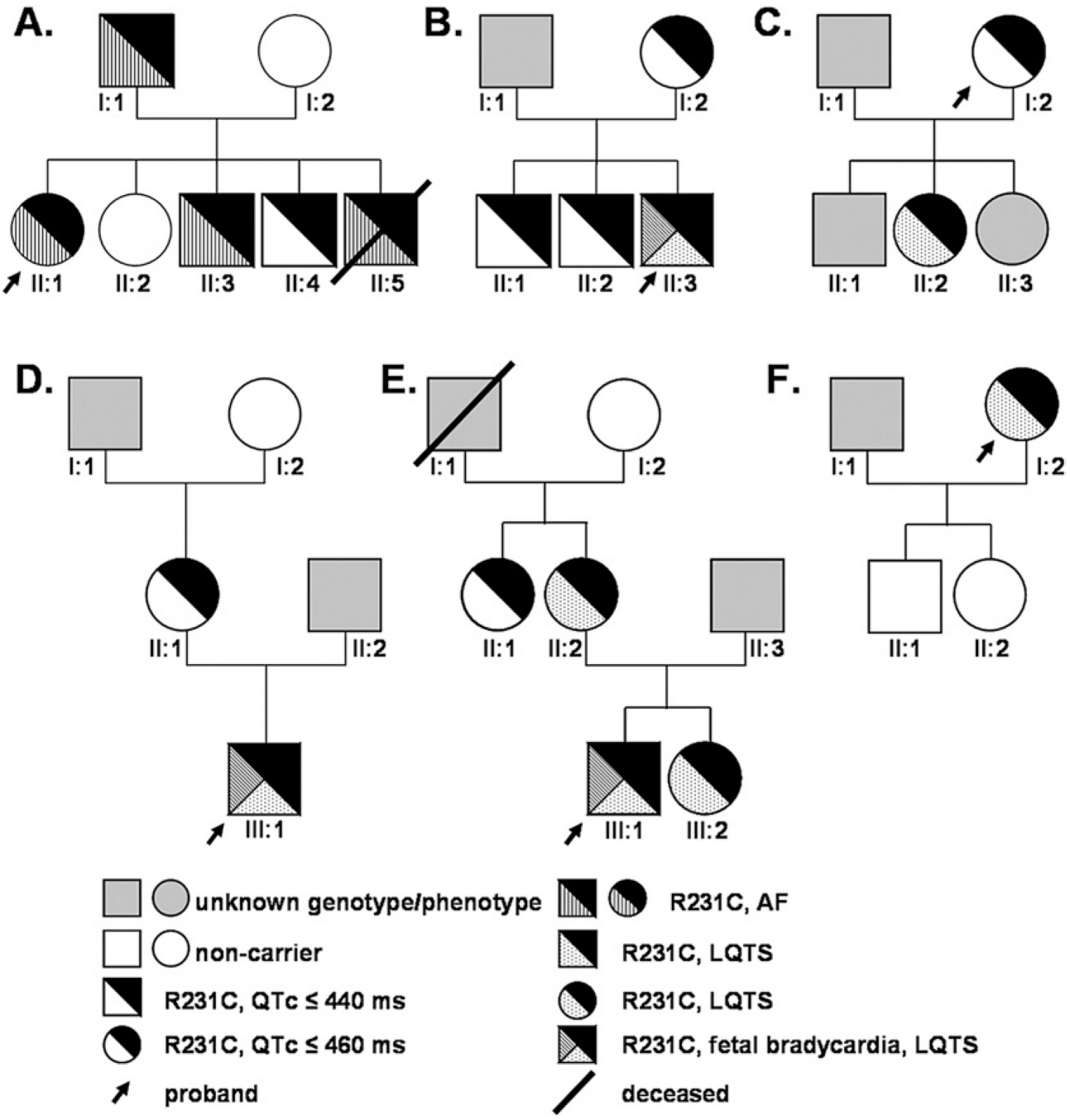

Figure 1.

Pedigrees of the six families carrying R231C-Q1. Males and females are represented as *squares* and *circles*, respectively. The different generations are denoted using roman numerals, and each individual in a generation is numbered. The genotype/phenotypes are defined in the key.

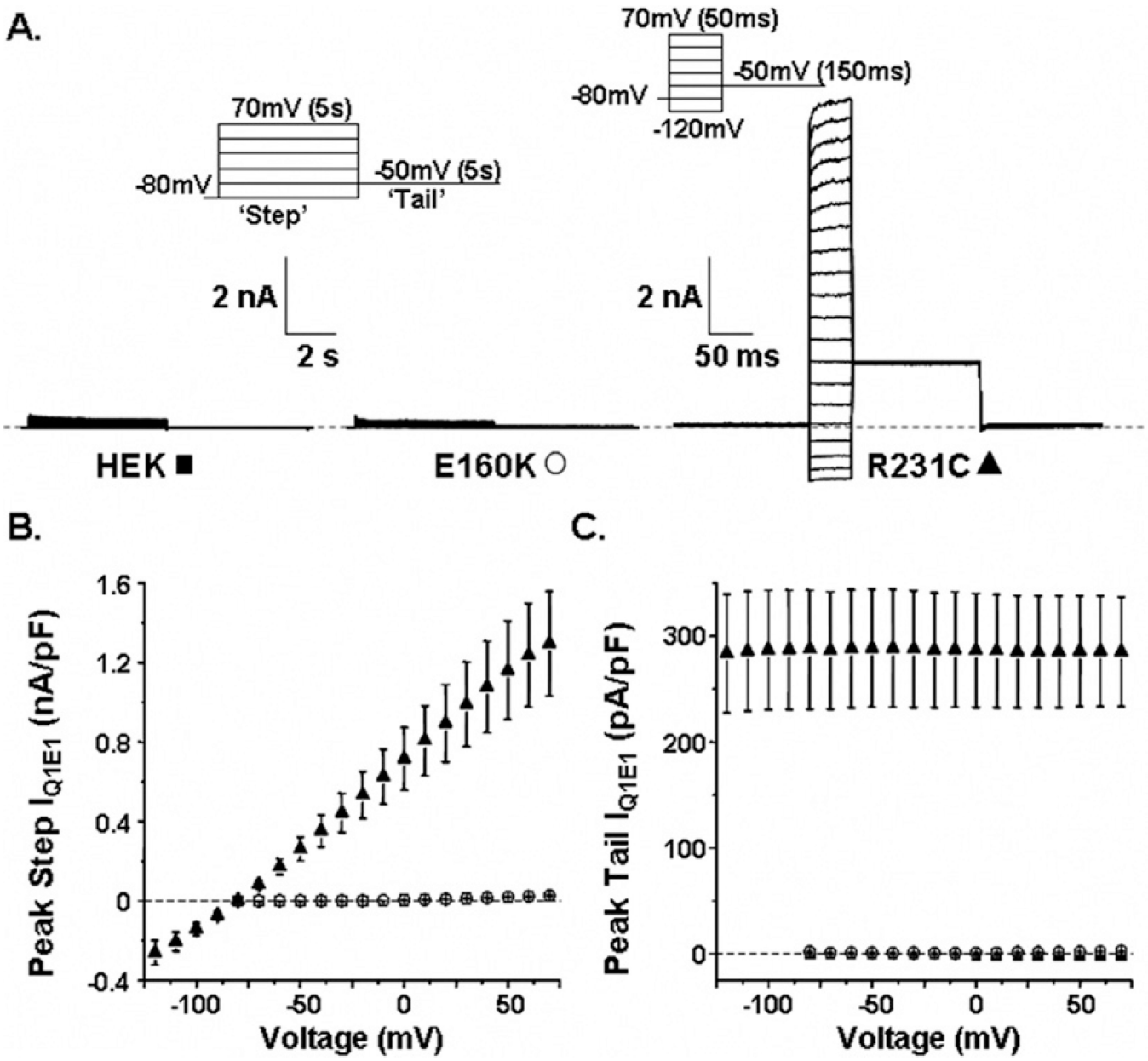

Figure 2.

A: Representative families of whole-cell currents recorded from nontransfected cells (HEK, ■), cells transfected with E1 and E160K-Q1 DNA (E160K, ○), or cells transfected with E1 and R231C-Q1 DNA (R231C, ▲). The corresponding voltage protocols used to measure the currents are also shown. Mean peak step (**B**) and tail currents (**C**) are plotted as a function of step voltage for nontransfected cells, cells expressing E160K-Q1, and cells expressing R231C-Q1.

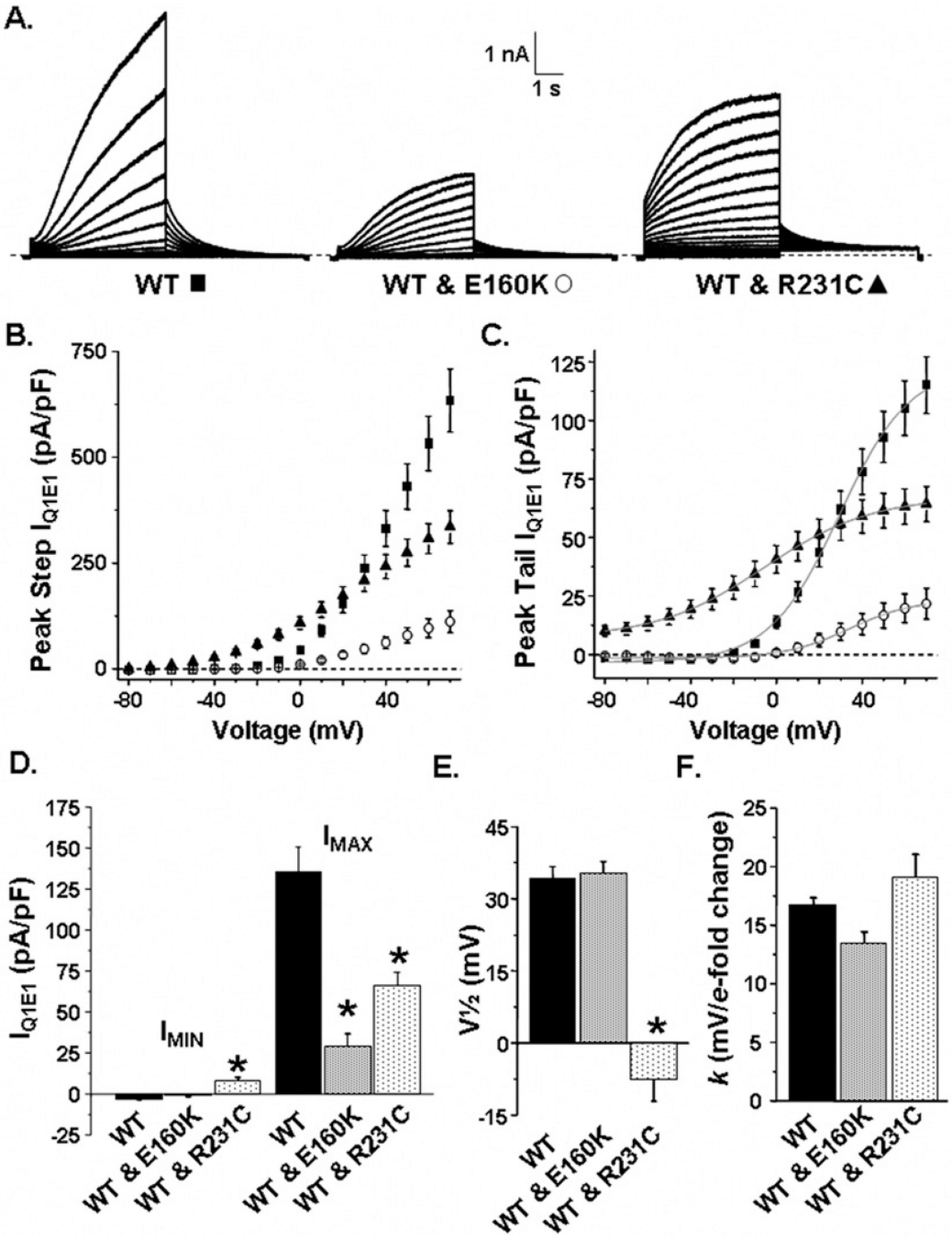

Figure 3.

A: Representative families of currents measured from cells transfected with E1 and WT-Q1 (WT, ■), WT-Q1 and E160K-Q1 (WT & E160K, ○), or WT-Q1 and R231C-Q1 DNA (WT & R231C, ▲). Mean peak step (**B**) and tail currents (**C**) are plotted as a function of step pulse for cells expressing WT-Q1, WT-Q1 and E160K-Q1, and WT-Q1 and R231C-Q1. Mean peak tail currents were measured immediately after the step pulse and were described using the Boltzmann equation *(gray line).* The graphs show the calculated mean I_{MIN} and I_{MAX} (**D**), $V_{1/2}$ (**E**), and slope constant, *k* (mv/*e*-fold change (**F**) for cells expressing WT-

Q1, WT-Q1 and E160K-Q1, and WT-Q1 and R231C-Q1. *P <.05 vs cells expressing WT-Q1.

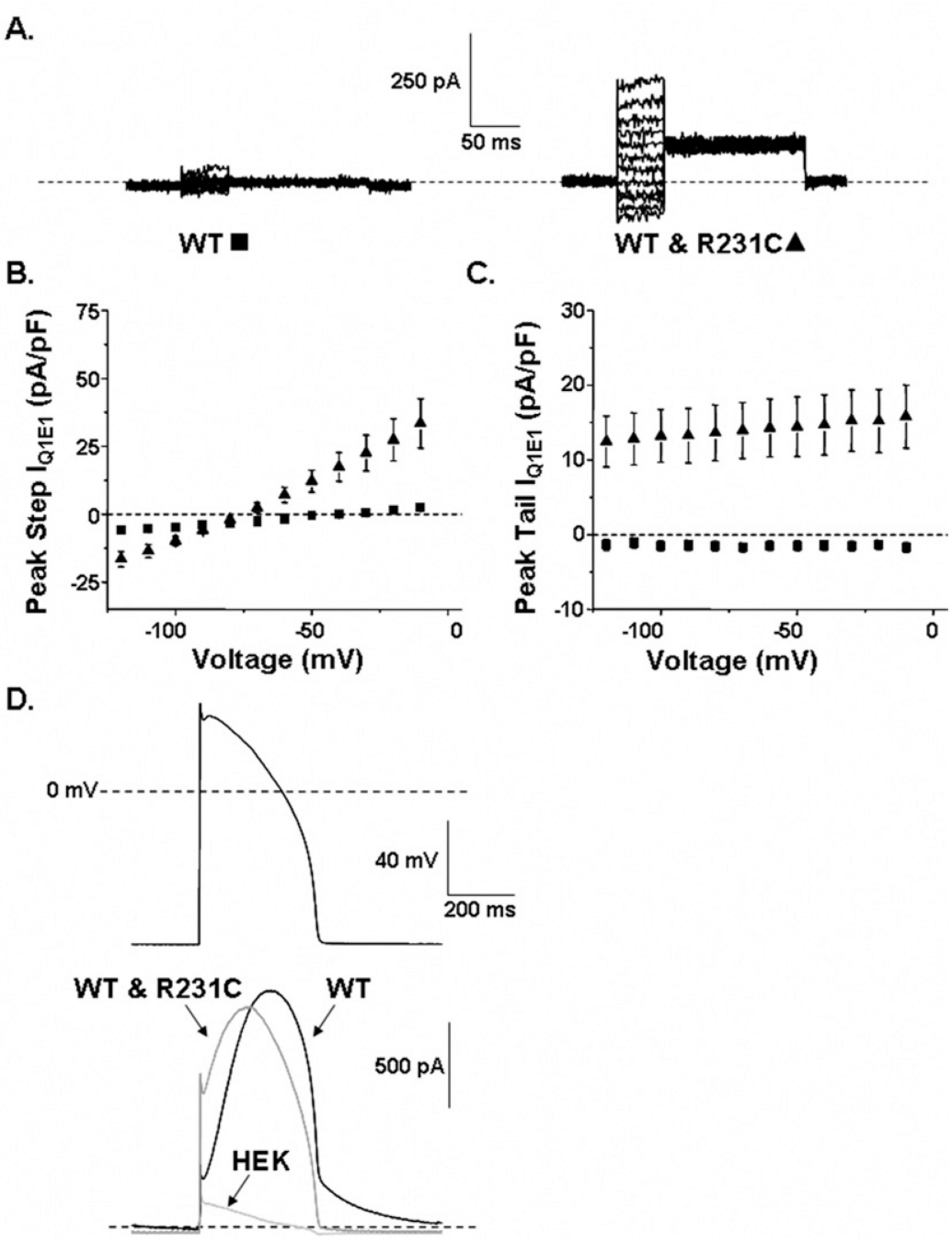

Figure 4.

A: Representative families of whole-cell currents recorded from cells transfected with E1 and WT-Q1 DNA (WT, ■) or WT-Q1 and R231C-Q1 DNA (WT & R231C, ▲). The currents were measured by applying step pulses from −120 to −10 mV for 50 ms, followed by a tail pulse to −50 mV for 150 ms. The corresponding mean peak step (**B**) and tail currents (**C**) are plotted as a function of step voltage. **D:** Ventricular action potential waveform and corresponding averaged current traces measured at 37°C from nontransfected (HEK) cells and cells transfected with E1 and WT-Q1 DNA or WT-Q1 and R231C-Q1 DNA.

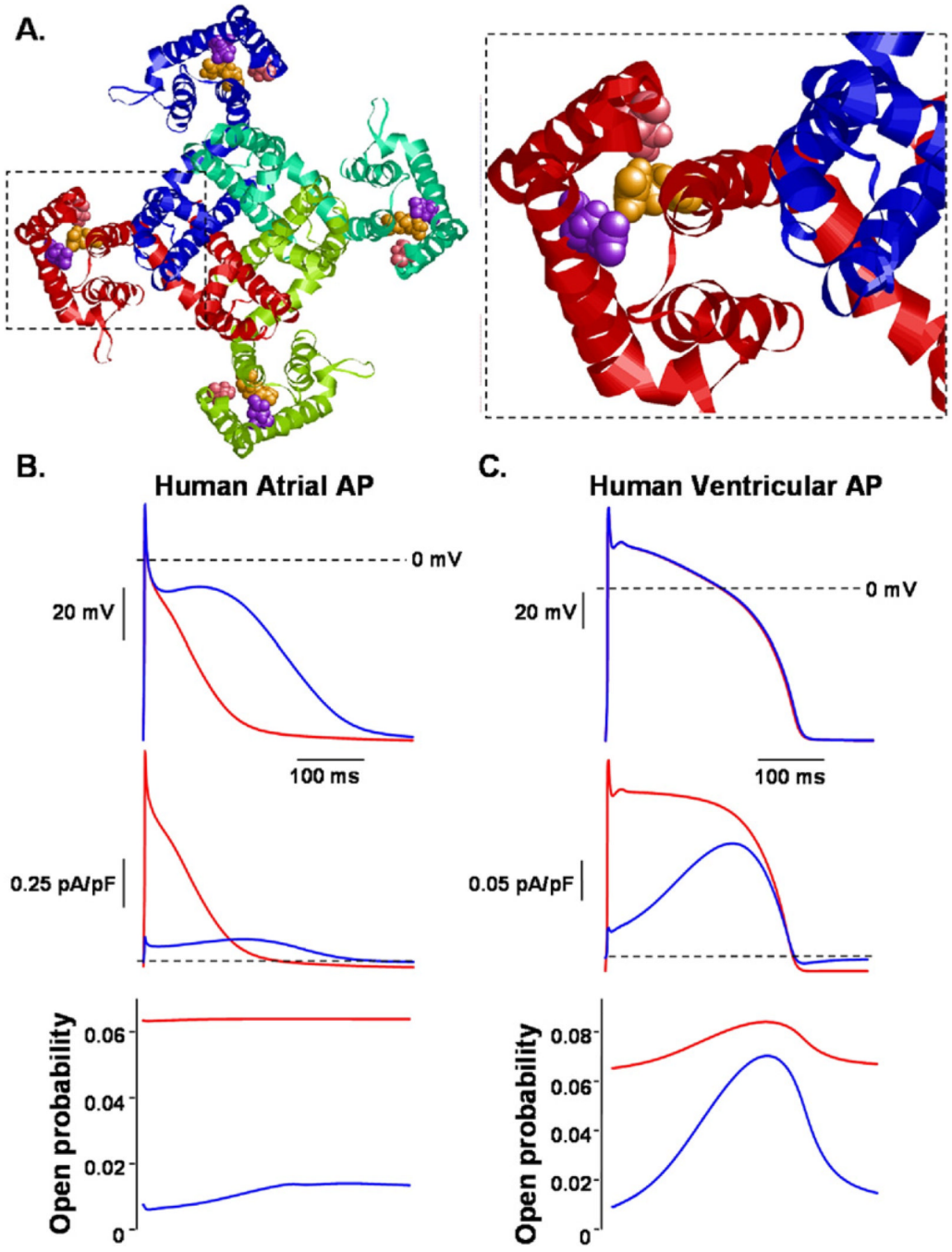

Figure 5.

A, left: Structural model of Q1 in the closed state from the "extracellular" side looking into the pore. The backbone of each individual Q1 α-subunit is shown as a different colored ribbon. The space filled atoms for the S140 *(pink)*, E160 *(purple)*, and R231 *(orange)* residues are shown in each α-subunit. **Right:** *Red* α-subunit magnified. The side chains of S140 and E160 are predicted to be close enough to form van der Waals contacts with R231 in the closed state. **B:** Computational model of a human atrial action potential (AP) waveform pulsed at 1 Hz with the corresponding I_{Ks} and channel open probability. *Blue traces* represent control conditions. *Red traces* show a modification of the model that

included a reduction in the number of functional channels by ~50% and a small constitutively active I_{Ks}. **C:** Computational model of a human ventricular AP pulsed at 1 Hz with the corresponding I_{Ks} and channel open probability. *Blue traces* represent control conditions. *Red traces* show a modification of the model that included the same reduction in functional channels and constitutively active I_{Ks} as shown in panel B.